Canadian Journal of Fisheries and Aquatic Sciences

OPEN ACCESS | Article

Using LASSO regularization to project recruitment under CMIP6 climate scenarios in a coastal fishery with spatial oceanographic gradients

Raymond Czaja, Jr.[a], **Daniel Hennen**[b], **Robert Cerrato**[a], **Kamazima Lwiza**[a], **Emmanuelle Pales-Espinosa**[a], **Jennifer O'Dwyer**[c], **and Bassem Allam**[a]

[a]School of Marine and Atmospheric Sciences, Stony Brook University, Stony Brook, NY 11790-5000, USA; [b]Northeast Fisheries Science Center, 166 Water Street, Woods Hole, MA 02543-1026, USA; [c]New York State Department of Environmental Conservation, East Setauket, NY 11733, USA

Corresponding authors: **Raymond Czaja, Jr.** (email: raymond.czaja@stonybrook.edu); **Bassem Allam** (email: bassem.allam@stonybrook.edu)

Abstract

As climate change disrupts fisheries, scientists are interested in fisheries projections under climate change scenarios. However, projections that account for spatial oceanographic gradients use increased variable selection power and output high spatial resolution climate data are needed to improve strategic fisheries management. This study uses the least absolute squares and selection operator, a regularization technique, and improved, climate change projections from phase 6 of the Couple Model Intercomparison Project to relate Atlantic surfclam, *Spisula solidissima solidissima*, recruitment to climate variables. Results show a longitudinal gradient in New York State waters where western recruitment displays a negative relationship with sea surface temperature and eastern recruitment displays a negative relationship with eastward spring wind intensity. Models project that recruitment in 2050 will decrease 100% in western waters and remain sporadic, but high, in eastern waters. This study provides insight regarding surfclam responses to climate change and considerations (methodological and statistical) for improved climate-based fisheries projections.

Key words: recruitment, LASSO, CMIP6, climate change, surfclam, oceanography

1. Introduction

As greenhouse gas emissions continue to alter the climate, there is a growing need to better understand the impact of climate change on fisheries. Time series analyses are frequently used to link interannual fisheries production (e.g., recruitment and stock size) to environmental variables such as sea surface temperature (SST) and climate indices (e.g., El Niño/Southern Oscillation Index) (Tian et al. 2003; Deyle et al. 2013; Bartolino et al. 2014; Miller et al. 2016). By establishing relationships between climate variables and fisheries production, it is then possible to project future production from climate model projections. While great progress has been made in climate-based fisheries projections, more precise and less biased projections are needed. Multidecade, climate-based projections are rarely used in tactical fisheries management, but improved strategic fisheries management stemming from more accurate climate-based projections can provide realistic expectations of stock trends through time under variable climate conditions (Myers 1998; Punt et al. 2014; Bell et al. 2018). Punt et al. (2014) identified directly linking fisheries production to Intergovernmental Panel on Climate Change (IPCC) models as a key factor when attempting fisheries projections in response to climate variables (termed the "mechanistic" approach in the context of using climate variation to aid fisheries management). Subsequently, recent work has incorporated climate projections in fisheries production models (Lehodey et al. 2013, 2015; Szuwalski et al. 2021). However, studies that have attempted projections may be limited by coarse climate projections that lack proper spatial resolution (Rheuban et al. 2017; Le Bris et al. 2018), and region-specific ocean climate change impacts (Brander 2010). New phase 6 Couple Model Intercomparison Project (CMIP6) Global Climate Model (GCM) output contains projections that are less biased (Séférian et al. 2020; Wang and Wang 2020) and more spatially resolute (Koenigk et al. 2020) than that of CMIP5, thereby potentially improving fisheries projections. For example, increased GCM resolution of 10 km has significantly decreased Spring SST bias in northwest Atlantic shelf waters (with zero bias in inner shelf waters in the Gulf of Maine and southern New England) (Saba et al. 2016). Only recently have CMIP6 GCM output been used in fisheries projections (Fauchald et al. 2021; Koul et al. 2021; Testa et al. 2022). Additionally, while previous fisheries models often include atmospheric forcing climate indices (e.g., ENSO and

NAO) (Brunel and Boucher 2007; Caputi et al. 2010; Muhling et al. 2018), models rarely include direct measures of wind in projections, which have been shown to explain interannual recruitment variation (Churchill et al. 2011; Hare et al. 2015; Skagseth et al. 2015) potentially due to larval transport and food supply mechanisms (Nakata et al. 2000; Vikebø et al. 2019). Although these indirect mechanisms are speculative, other studies have identified a need to include more fine-scale and specific predictors (e.g., individual wind vectors as opposed to climate indices) to improve precision, bias, and utility of projections (Brosset et al. 2020).

When working with a high number of predictor variables (e.g., SST and wind during multiple seasons), variable selection can be difficult. It is typical to construct models with all possible combinations of predictor variables and compare them using metrics such as Akaike information criterion (AIC) or AIC weights. However, this time-consuming approach can lead to the construction and comparison of over 100 models when just 12 predictor variables are used (A'mar et al. 2009). While functions such as the "dredge" function in R can help automate this process, as the function name implies, this approach is often criticized as data dredging (Anderson and Burnham 2004). Additionally, collinearity poses another issue when working with many predictor variables and has also been identified as an area of needed improvement in projecting fisheries recruitment from environmental factors (Myers 1998). Classic variable selection techniques such as stepwise regression aid in reducing the number of variables in the best-fit model but may yield other issues including parameter estimation bias, model selection algorithm inconsistencies, overfitting, and not utilizing the entire model space (Whittingham et al. 2006; Hegyi and Garamszegi 2011). Regularization techniques such as least absolute shrinkage and selection operator (LASSO) may not only solve the previously mentioned issues but also automate variable selection in one analysis and yield less prediction error than approaches such as stepwise regression (Kumar et al. 2019). Regularization differs from typical variable selection approaches in that it adds a shrinkage term to the model (Hastie et al. 2009). LASSO regularization differs from other regularization techniques (e.g., ridge regression) in that it attempts to shrink variable coefficients to zero (Tibshirani 1996) (i.e., ridge regularization retains all variables since coefficients are not shrunk to zero but LASSO removes unnecessary variables that yield coefficients that may be shrunk to zero). Furthermore, regularization techniques such as LASSO may account for collinearity among predictor variables and sample the whole model space, increasing their utility in fisheries ecology which often yields situations with a high total number of variables and many collinear variables (Tibshirani 1996; Hastie et al. 2009; Gownaris et al. 2018; Plumpton 2018). LASSO is common in medical (Kidd et al. 2018; McEligot et al. 2020) and bioinformatics (Li et al. 2011; Lu et al. 2011) literature, but has yet to be applied to fisheries projections.

The Atlantic surfclam, *Spisula solidissima solidissima*, is among many fisheries in the northwest Atlantic that have been shown to be negatively impacted by climate change. Surfclams are large (upto 30 cm long) (Weinberg 1999) bivalves found in soft-sediment, inner-shelf waters (10–50 m) and are distributed between the Gulf of St. Lawrence and Cape Hatteras (Wigley and Emery 1968) where they support a multimillion dollar industry. In many areas, including New York State (NYS) waters, populations have experienced large (>70%) declines in recent decades (Dahl and Hornstein 2010; O'Dwyer and Hornstein 2013). Fishing mortality is well beneath overfishing thresholds (NEFSC 2017). However, increased temperature has been linked to distributional shifts to cooler waters (Weinberg 2005), low condition indices (Marzec et al. 2010), low assimilation rates (Narváez et al. 2015), low scope for growth (Hornstein et al. 2018), low growth rates (Munroe et al. 2016), and gonad abnormalities (Kim and Powell 2004). O'Dwyer and Hornstein (2013) demonstrated a sharp decrease in prerecruit surfclams (i.e., individuals that had not yet recruited to the fishery) from 2002 to 2012, suggesting recruitment failure may also be contributing to population declines. Surfclam recruitment and larvae settlement are notoriously patchy in time and space and are thought to be influenced by abiotic (hydrodynamics, wind, and temperature) and biotic factors (predation and food availability) (Chintala and Grassle 2001; Ma and Grassle 2004; Ma 2005; Ma et al. 2006). Better understanding the impact of these factors on surfclam recruitment is particularly important for projecting recruitment, as climate change continues to increase coastal SST, alter wind and current patterns (Harley et al. 2006), and affect bivalve food availability (Boyce et al. 2010; Winder and Sommer 2012).

In NYS waters (representing close to the mean latitude within surfclam distribution) mean summer SST of surfclam habitat has increased over 2 °C from the late 1980s to the late 2010s (NOAA Buoy 44025). Mean summer SST now regularly exceeds 23 °C, a known physiological thermal threshold for surfclams (Kim and Powell 2004; Narváez et al. 2015; Hornstein et al. 2018), thereby providing a mechanism by which SST may be negatively affecting recruitment. Establishing a mechanistic basis for models that link climate variables to fisheries recruitment has not only proven vital for improved tactical management (Guisan and Zimmermann 2000; Dickey-Collas et al. 2014; Maunder and Thorson 2019), but may yield relationships that are more likely to hold up through time, thereby also improving strategic management. Therefore, the NYS surfclam fishery represents an ideal case to study climate–recruitment relationships. Additionally, spatial oceanographic gradients (e.g., warmer, higher chlorophyll waters in the west and cooler, lower chlorophyll waters in the east) (O'Reilly and Zetlin 1998) in NYS waters suggest potential spatial variation in climate–recruitment relationships. Accounting for spatial oceanographic gradients in climate–recruitment relationships is not always implemented (Keyl and Wolff 2008), but when accomplished, has revealed important relationships that change in space and increase predictive power (Wolff and Vargas 1994; Planque and Frédou 1999).

In a review of fisheries environment–recruitment relationship studies, Myers (1998) emphasizes multiple approaches to improve the field including testing general hypotheses that function more than a simple case study. In the present study, the general hypotheses of (1) the presence of spatial

gradients in recruitment–climate relationships, (2) a negative SST–recruitment relationship due to thermal stress, and (3) the presence of wind–recruitment relationships due to potential wind influence on larval transport or food availability are tested. While testing these hypotheses may not yield information for immediate use in tactical management, unraveling these relationships may lead to improved strategic management. Surfclams are used here as a model species; however, these general hypotheses can be applied to other temperate, coastal fisheries. Increasing SST patterns, spatial oceanographic gradients, and a declining fishery create a need to unravel climate-recruitment relationships and to project future recruitment for surfclams. This need presents an ideal opportunity to apply LASSO and updated CMIP6 GCM output for fisheries projections. The objectives of the present study were to (1) establish temporal and spatial recruitment trends in the NYS surfclam fishery, (2) determine which climate variables significantly impact surfclam recruitment using LASSO, and (3) create projection models using CMIP6 GCM output.

2. Methods

2.1. Recruitment estimates

Surfclam population data were obtained from the New York State Department of Environmental Conservation surveys from 1999, 2002, 2005, 2006, 2008, and 2012. Data from previous surveys were available but were omitted, as earlier surveys were conducted without a dredge mesh liner to capture smaller sized clams. Survey method details can be found in Dahl and Hornstein (2010). In short, a hydraulic dredge was used to catch adult surfclams from 238 randomly selected stations per survey in a stratified sampling design within NY state waters between Rockaway Inlet (40°34′55.0″N, 73°45′18.0″W) and Montauk Point (41°04′13.0″N, 71°51′20.2″W). Catch per unit effort (CPUE) were reported in bushels and specified for age classes. Ages were estimated by counting annual growth lines from chondrophore cross-sections. CPUE for each age class was corrected for mortality as follows:

$$\text{Mortality Adjusted CPUE} = \text{CPUE}\left(\frac{1}{e^{(-0.15 * X)}}\right)$$

where X is the number of years past recruitment for that cohort. A mortality value of 0.15 year^{-1} was chosen as a stock standard mortality value (NEFSC 2017). Mortality was initially estimated via catch–curve analyses; however, unreasonable mortality values suggested that the data may be too noisy to allow direct mortality estimation. CPUE data (for each age class) were explored via a bubble plot to help gauge general temporal and spatial trends in biomass.

Young of the year estimates were not provided from surveys and multiple year gaps existed between surveys; therefore, direct estimates of annual recruitment were unavailable. Instead, a mean cohort strength index (CSI) was developed as a relative proxy for annual recruitment. CSI values are not intended as an absolute measure of recruitment, but are presented to allow comparison of recruitment strength between years, such that a positive CSI value represents a (birth) year with above average recruitment and a negative CSI value represents a year with below average recruitment. Due to low catchability and aging inaccuracy for young clams, clams younger than 4 years were not used in analyses. CSI values were calculated as follows:

$$\text{CSI}_{t,i} = \frac{\text{CPUE}_{t,i} - \mu_i}{\sigma_i}$$

where CPUE is mortality-adjusted CPUE, μ is mean catch, σ is catch standard deviation, t is year of birth, and i is survey year. Therefore, each year class yielded multiple CSI values based on the number of surveys that captured that year class. For example, the 1994 year class was captured by six surveys yielding six CSI values, and the 2004 year class was captured by two surveys yielding two CSI values. The mean CSI value for each year class was calculated and used as a relative proxy for recruitment for a given year class. Year classes with less than two CSI estimates were not included in analyses due to uncertainty associated with only one CSI value and CSI estimates from individuals older than 20 years old were not included due to senescence mortality, yielding $n = 18$ from 1987 to 2004. Survey catch data are typically reported within four longitudinal strata: Rockaway Inlet to Jones Inlet (RJ), Jones Inlet to Fire Island Inlet (JF), Fire Island Inlet to Moriches Inlet (FM), and Moriches Inlet to Montauk Point (MM) (see Dahl and Hornstein (2010) for precise, visual displays of strata locations). CSI values were initially calculated for each longitudinal stratum but a Spearman correlation revealed a significant correlation between RJ and JF CSI values ($p = 0.0086$). Therefore, catch data for RJ and JF were combined for CSI calculations, yielding CSI values for three different longitudinal regions (Fig. 1).

2.2. Variable selection

To obtain SST values for each region, SST daily data were downloaded from the Group for High-Resolution Sea Surface Temperature (GHRSST) database (https://www.ncei.noaa.gov/thredds-ocean/catalog/ghrsst/L4/catalog.html) and averaged into monthly bins. These data are produced on a 0.25° grid and represent temperature from the surface to 10 m. For each region, the grid point closest to the region center was chosen for region-specific SST values (Fig. 1). Wind data were obtained from the National Data Buoy Center (NDBC) buoys and C-MAN stations. Data were obtained from NDBC Buoy 44025 and when data were missing, data were taken from Ambrose Light Tower, Buoy 44065, and Buoy 44017. Unlike SST, which included region-specific data, wind data from NOAA buoys were applied to all three regions uniformly. Mean seasonal SST, east–west wind components (U), and north–south wind components (V) were calculated as follows: Winter is the mean of January 1st to March 31st; Spring is the mean of April 1st to June 30th; Summer is the mean of July 1st to September 30th; and Fall is the mean of October 1st to December 31st. Seasonal SST and wind component anomalies were then calculated (as deviations from seasonal means from 1987 to 2004) and used for variable selection and model construction. U and V wind components

Fig. 1. Three longitudinal regions, each with independent annual surfclam cohort strength index (CSI) trends, in New York State waters. Black stars represent locations for region-specific SST data. This map (projected coordinate system) was created via shoreline data from the Global Self-consistent, Hierarchical, High-resolution Geography Database (https://www.soest.hawaii.edu/pwessel/gshhg/) using the R package "rnaturalearthhires" v0.2.0.

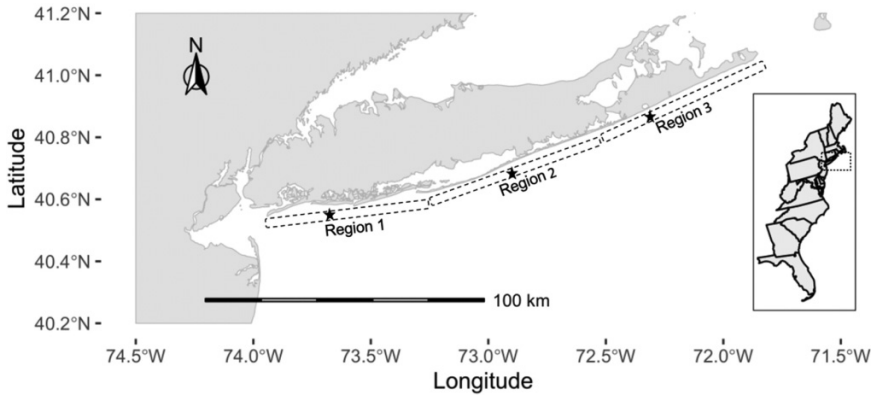

were calculated by multiplying the sine and cosine, respectively, of wind direction (radians) by wind speed ($m \cdot s^{-1}$). Therefore, a positive U value represents an eastward wind, a negative U value represents a westward wind, a positive V represents a northward wind, and a negative V represents a southward wind.

LASSO was used for preliminary variable selection in model construction. In MATLAB, the "lasso" command (maximum likelihood estimation) was used such that retained variables had nonzero coefficients associated with the lambda (cutoff) value that resulted in the lowest mean squared error (LMSE) after leave-one-out cross-validation (LOOCV). In other words, the lambda at the LMSE was the chosen lambda. This approach has proven successful with preventing overfitting with small data sets, as is the case in the present study (Dahlgren 2010), as all lambda values up to 100 are explored, and the higher the lambda, the greater the penalty. For a given lambda, LASSO estimates variable coefficients by solving for the equation (matrix notation):

$$\text{Lasso MSE} = \min_{\beta_0 \beta} \left(\frac{1}{2N} \sum_{i=1}^{N} \left(y_i - \beta_0 - x_i^T \beta \right) \right)^2 + \lambda \sum_{j=1}^{p} |\beta_j|$$

where β and β_0 are the regression coefficients of scalar length p, N is the number of observations, y is the response variable at observation i, x is the predictor variable of vector length p and at observation i, and λ is shrinkage penalty parameter. To account for the possibility that mean CSI values may lack precision, in terms of estimating annual recruitment, weights were applied to CSI values for LASSO. CSI weights were calculated as the number of surveys that capture a particular year class. This approach gives more weight to CSI means that were calculated from a higher number of surveys, thereby removing predictor variables that may otherwise be retained due to spurious correlation with noisy CSI values. Variables retained by LASSO were then used in the second step of model construction where CSI weights were also applied.

2.3. Model construction and selection

Following LASSO variable selection, multiple candidate models were constructed for each region such that CSI values were predicted as a linear function of different subsets of LASSO selected variables. Backward stepwise selection was used to remove LASSO selected variables to create parsimonious subsets of variables such that for each region the first subset included all LASSO selected variables and the last subset included the last remaining variable. This approach generated one candidate model for Region 1, four candidate models for Region 2, and three candidate models for Region 3. Generalized additive models (GAMs) were also explored, but were ultimately excluded from model selection for numerous reasons (see the supplementary material for further discussion).

To select the best candidate model for regional projections given the data, AIC values, residual standard errors (RSEs), and R-Squared values of original models and LOOCV analyses were calculated and assessed. LOOCV procedures have been shown to provide unbiased estimates of model prediction accuracy, even at small sample sizes (Olden and Jackson 2000). For LOOCV analyses, one observation was left out of the data set to obtain a training model of $n = 17$. The missing observation was then predicted from that model. This was repeated for each observation. As the primary assessment for model selection, the LOOCV R-Squared value trends were analyzed. More specifically, as the number of predictor variables increased, the LOOCV R-Squared value trend was analyzed to see whether the LOOCV R-Squared value continued to increase as the number of predictor variables increased (i.e., at which model did LOOCV R-Squared value peak) (Flanagan and Cerrato 2015). The candidate model that yielded the highest LOOCV R-Squared value is suggested to yield the highest prediction accuracy. However, because the trend (i.e., peak) of LOOCV R-Squared values was unclear for Region 3 (see the "Results" section), a second assessment for model selection was also considered. For the second assessment, the % difference in RSEs between the original model-fitted values and the fitted values of the LOOCV model

(hereafter referred to as RSE % difference) was then assessed, such that a smaller RSE % difference means higher prediction accuracy of the original model. Model assumptions and diagnostics were inspected when appropriate. Model construction and assessments were conducted in R Version 4.0.2 using base packages, the "mgcv" package (R Core Team 2020), "caret" package (Kuhn 2008), and the "SardineForecast" package (Holmes 2020). Maps were created in R Version 4.0.2 using the "rnaturalearthhires" package (South 2023) and GSHHG shapefile data (Wessel and Smith 2017) and in MATLAB using the "M_Map" package (Pawlowicz 2020).

2.4. Projections

Projecting of CSI values was conducted across two time periods: (1) from 2005 to 2019, when observational data were available and (2) from 2020 to 2050, when GCM data were incorporated. For the first part SST (GHRSST) and wind (buoy) data were imported as previously described into the selected models for each region as predictor variables. For the second part, GCM output from CMIP6 simulations were used. This new generation of GCM simulations not only allowed for climate output at higher resolutions but also decreased GCM bias (see the "Discussion" section for appropriate GCM context). The simulations used in the present study included Socioeconomic Pathway 5 (SSP5), which is close to the Representative Concentration Pathway 8.5 (RCP 8.5). An SSP5 scenario assumes no mitigation (Riahi et al. 2011) and increasing gas emissions overtime under projected global population growth (IPCC 2014). GCM output was obtained online via the CMIP6 data portal (https://esgf-node.llnl.gov/search/cmip6/). For SST projections (identified as tos in GCMs), output from five GCMs were used. These GCMs were chosen because they meet our spatial resolution requirements (≤25 km). Additionally, these GCMs have been previously used for ecological projections and/or their tos output for the north Atlantic had been assessed by previous climate studies (Table S1). Wind projections, (with standard GCM variable names uas and vas for east and north component, respectively) output were used from three GCMs. These GCMs were chosen as they were the only available GCMs (with uas and vas output) that met spatial resolution requirements (≤25 km) (Table S1). For each GCM, values were selected at a grid point that was nearest to the center of each region. GCM output were calibrated (from 1987 to 2014) for each region using the bias correction method (Ho et al. 2012). For each output variable, bias corrected values were averaged across all GCMs. These data were then imported as previously described into the selected models for each region as predictor variables.

Additionally, to visualize GCM projections relative to present day, SST and wind vectors during seasons of interest were averaged from 2015 to 2024 and 2041 to 2050 and displayed and compared via maps (Figs. S1 and S2). For maps, SST projections from the NCAR.CESM1-CAM5-SE-HR model and wind projections from the CAS.FGOALS-f3-H were used as these GCMs contained the highest resolution and produced values close to the average of all GCMs used.

Fig. 2. Winter (A), spring (B), summer (C), and fall (D) sea surface temperature data (obtained from the Group for High-Resolution Sea Surface Temperature) for three longitudinal regions (with Region 1 being the western most region and Region 3 being the eastern most region) from 1987 to 2019.

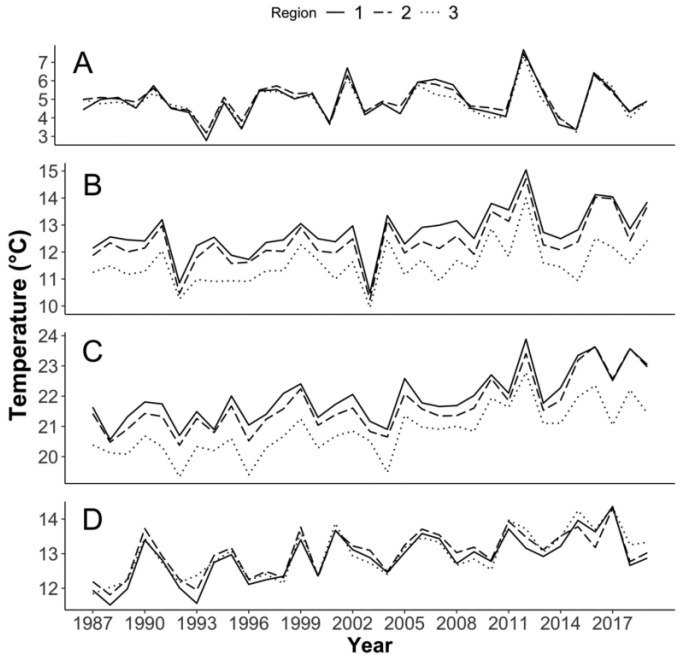

3. Results

3.1. Climate variables

Seasonal SSTs generally increased from 1987 to 2019 (Fig. 2). For example, mean Spring and Summer SST (Region 1) of the first decade (i.e., 1987–1996) and the last decade (i.e., 2010–2019) increased 1.3 and 1.5 °C, respectively (Figs. 2B and 2C). During years for which observed CSI values are available, particularly warm years occurred in 1995 and 1999 (Fig. 2). During years for which CSI values were projected, particularly warm years occurred in 2012 and 2016 (Fig. 2). The summer east component of wind, SummerU generally decreased from 1987 to 2019, but no directional patterns were observed for other seasonal Us (Fig. 3). Most years for all seasons resulted in positive Us (i.e., winds blowing to the east) (Fig. 3). WinterU and FallU averages were never negative, but SpringU and SummerU were occasionally negative, such as in 1992 and 2009 (Fig. 3). No directional changes were observed for seasonal north component Vs from 1987 to 2019 (Fig. 3). SpringV and SummerV were generally positive (i.e., winds blowing to the north); however, occasional negative SpringVs occurred, such as in 1991 and 2003 (Fig. 3). WinterV and FallV were generally negative (i.e., winds blowing to the south); however, occasional positive WinterVs and FallVs were experienced, such as in 1997 and 2001, respectively (Fig. 3).

3.2. Catch data

Catch data not only displayed decreasing CPUE through time but also showed sporadic changes in CPUE between age

Fig. 3. U wind component (A) and V wind component (B) from NOAA buoys near New York State waters from 1987 to 2019.

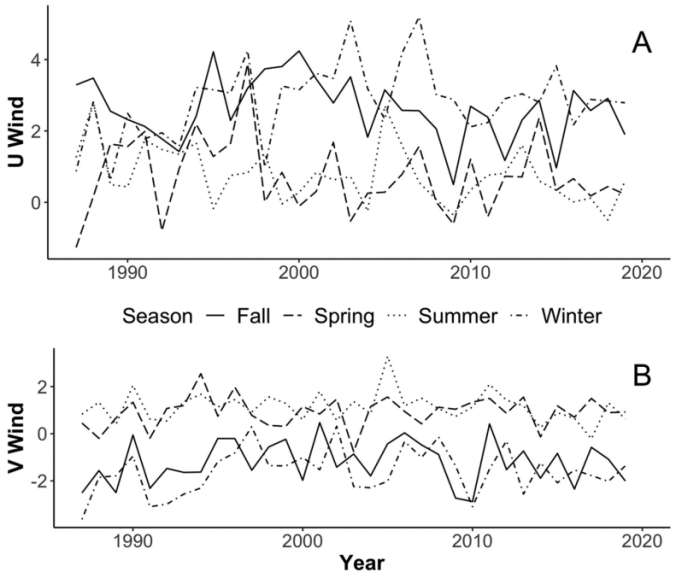

classes, suggesting episodic recruitment (Fig. 4). CPUE in Regions 1 and 2 was generally greater than that in Region 3, as suggested by the larger bubbles and larger bubble scaling factors in Regions 1 and 2 (Fig. 4). Bubble plots suggested that the data performed adequately in terms of tracking large cohorts through time. For example, in Region 2, relative to other cohorts within each survey year, the age 7 year class of 1999, age 10 year class of 2002, age 13 year class of 2005, and age 14 year class of 2006 were relatively large (Fig. 4). Furthermore, CPUE for that age class appeared to be slightly decreasing through time, suggesting detectable mortality (Fig. 4).

3.3. Observed CSI patterns and LASSO results

All three regions began the time series with positive CSI values, suggesting an above average recruitment year (Fig. 5). Region 1 experienced generally decreasing CSI values until 2004, with the exception of a CSI spike from 1995 to 1997 (Fig. 5A). Region 2 also experienced generally decreasing CSI values, with the exception of a CSI spike in 1992 (Fig. 5B). Region 3 also experienced a CSI spike in 1992, but it experienced generally increasing CSI values after 1998 (Fig. 5C). CSI confidence intervals for Region 3 appear wider than Regions 1 and 2 (Fig. 5), likely because Region 3 experienced lower surfclam abundances and catches (Fig. 4). LASSO retained one predictor variable for Region 1, zero predictor variables for Region 2, and three variables for Region 3 (Table 1). A temperature variable was only retained for Region 1, which yielded a negative relationship with CSI values (Table 2). Wind variables were only retained for Region 3, all of which yield negative relationships with CSI values (Table 2). LASSO yielded an oceanographic gradient where temperature variables were more important in the west (e.g., Region 1) than the east (e.g., Region 3) and wind variables were more important in the east than the west. Furthermore, LASSO yielded no positive relationships between temperature variables and CSI values in any region and yielded positive relationships with eastward winds in the western regions during the spawning season (Spring and Summer). Because LASSO did not retain any variables for Region 2 (see the "Discussion" section for more explanation), the last four variables to be eliminated by LASSO were used to create candidate models, including FallT, FallV, WinterV, and SummerU (Table 3). Therefore, Region 2 overlaps with Region 1 in that FallT was included in candidate models, and Region 2 overlaps with Region 3 in that WinterV and spawning season U winds (SummerU and SpringU) were included in candidate models (Tables 3).

3.4. Region 1 model selection and projections

For Region 1, only one variable (FallT) was retained by LASSO; therefore, only one candidate model was considered for Region 1 (Table 3). Both the Model R-Squared and RSE % differences were relatively low. While the low Model R-Squared suggests poor explanatory power, the low RSE % difference suggests adequate predictive power (see the "Model construction and selection" section for discussion and hierarchy of model selection measures). Diagnostics for Model 1 did not display strong evidence for departures from normality and linearity and yielded no Cook's distance values greater than 1.0 (Fig. S3). Unsurprisingly, Part 1 and Part 2 projections yielded consistently negative and declining CSI values (Fig. 6A), due to increasing FallT trends, as FallT projections yielded increases of ~1.5 °C between the beginning and end of Part 2 projections (Fig. S1). While model uncertainty is noticeably higher after 2030, confidence intervals rarely extend above zero, suggesting reliable projections of low recruitment (Fig. 6A). A notable drop in projected CSI values was observed in 2040, due to GCM projections of an anonymously warm year (Fig. 6A). From 2041 to 2050, Part 2 projections yielded a mean CSI value of approximately −1.14, corresponding with a 100% decrease in CPUE relative to the average of all the observed values.

3.5. Region 2 model selection and projections

Parsimonious subsetting yielded four candidate models for Region 2 (Table 3). Linear model coefficients for each variable from the least parsimonious model are as follows: SummerU = 0.342, WinterV = −0.230, FallV = −0.157, and FallT = −0.245. All four models yielded relatively high R-Squared values and AIC values that never differed by more than 2.0 (Table 3). The LOOCV R-Squared value peaked for Model 2 (i.e., with three predictor variables) and declined at Model 1 (i.e., with all four predictor variables), suggesting the highest predictive accuracy for Model 2 (Table 3). Therefore, Model 2 was chosen for projections (Table 3). It should be noted that while the primary assessment of prediction accuracy (i.e., the LOOCV R-Squared trends) suggested highest predictive accuracy for Model 2, the RSE % difference (i.e., the secondary assessment of prediction accuracy) was the lowest for Model 4 (Table 3). Similar to Region 1, the model with the highest predictive accuracy (Model 2) included FallT (Table 3). Model 2 also included SummerU and WinterV. Diagnostics again did not display strong evidence for departures from normality and linearity and yielded no Cook's distance values greater

Fig. 4. Bubble plot displaying catch per unit effort (CPUE) of individual cohorts from each survey for Region 1 (A), Region 2 (B), and Region 3 (C). Legends display region-specific scaling factors for bubble sizes and minimum, median, and maximum CPUE.

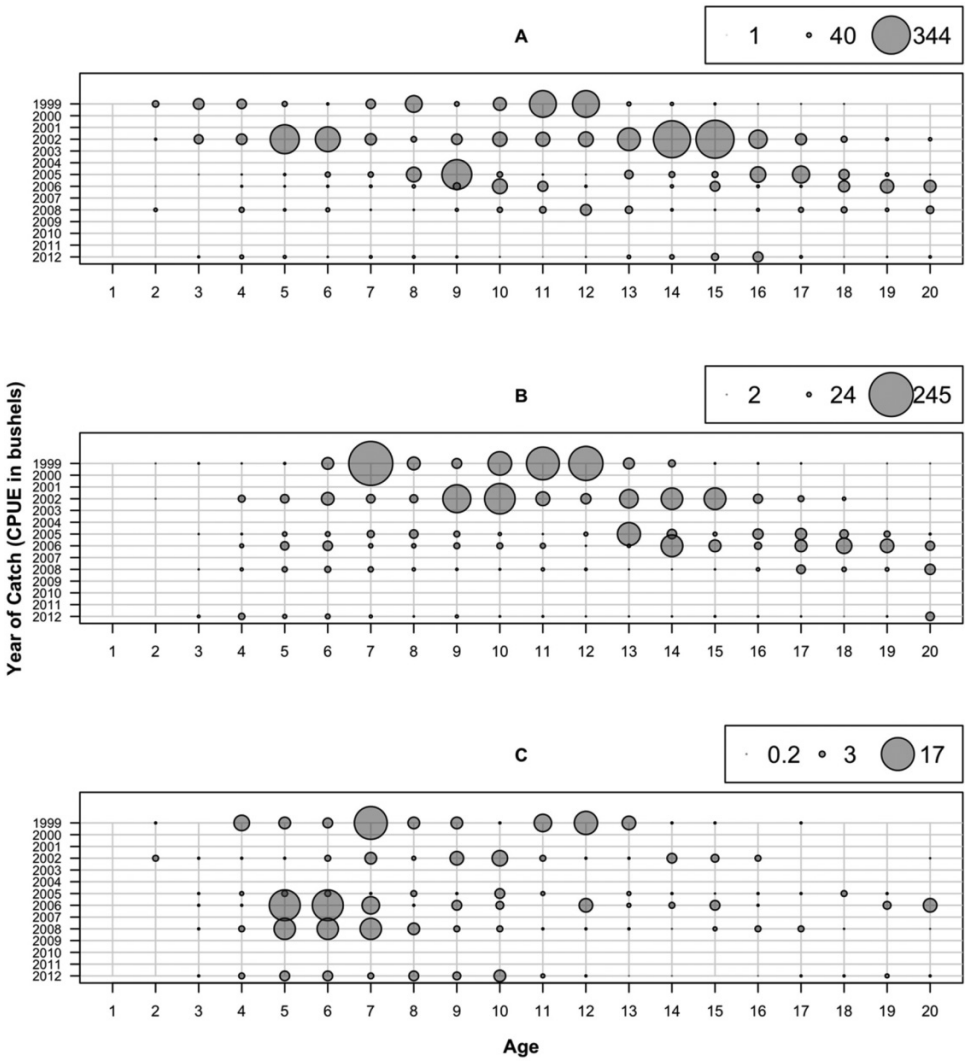

than 1.0 (Fig. S4). Also, similar to Region 1, Part 1 CSI projections yielded generally decreasing CSI values and Part 2 projections yielded consistently negative and declining CSI values (Fig. 6B) due to increasing FallT trends (Fig. 6B). Both projection parts yielded sporadic CSI spikes during years with cool Falls, strong Summer winds from the west, and strong Winter winds from north (Fig. 6B). Model uncertainty is again noticeably higher after 2030 (Fig. 6B). However, unlike Region 1, confidence intervals for Region 2 occasionally extend above zero, suggesting potential high recruitment during years with strong Summer winds from the west and strong Winter winds from north (Fig. 6). From 2041 to 2050, Part 2 projections yielded a mean CSI value of approximately −1.54, corresponding with a 100% decrease in CPUE relative to the average of all the observed values.

3.6. Region 3 model selection and projections

Parsimonious subsetting yielded three candidate models for Region 3 (Table 3). The least parsimonious model (i.e., Model 1) yielded a relatively high Model R-Squared value, but the most parsimonious model yielded a relatively low Model R-Squared value (Table 3). All three models yielded AIC values that never differed by more than 1.5 (Table 3). The LOOCV R-Squared value decreased when one predictor variable was removed but then increased when two predictor variables were removed (i.e., Model 2 has the lowest LOOCV R-Squared but Model 3 has the highest LOOCV R-Squared) (Table 3). The unclear LOOCV R-Squared trend allowed for precedence of RSE % difference assessment in choosing the best model for projections (Table 3). Model 3, the most parsimonious model, had the lowest RSE % difference, suggesting the greatest predictive accuracy (Table 3). Therefore, Model 3, which only included SpringU, was chosen for projections (Table 3). For Model 3, diagnostics again did not display strong evidence for departures from normality and linearity and yielded no Cook's distance values greater than 1.0 (Fig. S5). Part 1 projections yield sporadic CSI values with minor spikes but Part 2 projections yield consistently positive CSI values with great spikes (Fig. 6C), due to SpringU winds that fluctuated but gradually became more negative (Fig. S2). Model uncertainty was considerably lower for Region 3 than Regions 1 and 2 (Fig. 6). From 2041 to 2050, Part 2 projections yield a mean

Fig. 5. Observed annual cohort strength index (CSI) trends for Region 1 (A), Region 2 (B), and Region 3 (C) from 1987 to 2004. Shaded regions represent 95% confidence intervals.

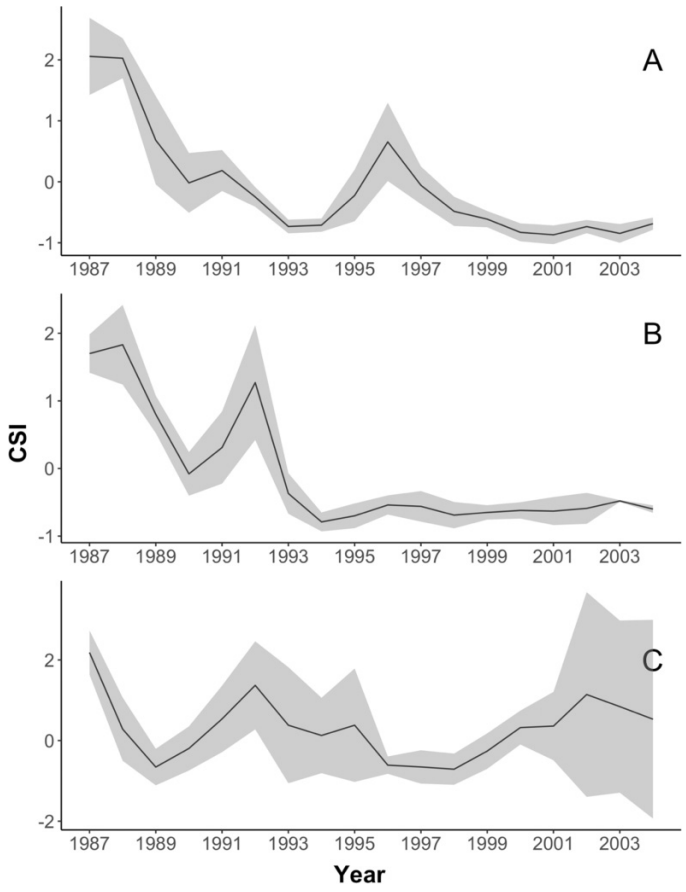

Table 1. Least absolute shrinkage and selection operator output for each region.

Region	Variables retained	Lambda	LMSE
1	FallT	0.3442	97
2	N/A	0.4942	100
3	SpringU, WinterV, SummerV	0.1306	87

Note: Variables retained had nonzero coefficients at the lambda value associated with the lowest mean squared error (LMSE).

CSI value of approximately 0.32, corresponding with a 2% increase in CPUE relative to the average of all the observed values.

4. Discussion

4.1. General model performance

These results demonstrate that LASSO can prove a valuable tool in constructing models that project fisheries metrics in response to climate change and nonanthropogenic environmental variability. Additional variable subsetting was needed after LASSO, and LASSO did not retain variables for Region 2 (see the next paragraph). However, LASSO helped to unravel region-specific relationships between surfclam recruitment and climate variables that are likely due to spatial gradients in oceanographic conditions. These relationships suggest that ocean warming is driving recruitment failure in western NYS waters and that Winter and spawning season (i.e., Spring and Summer) wind patterns drive episodic recruitment in eastern NYS waters.

Interestingly, LASSO did not retain any variables for Region 2. One potential reason is that Region 2 is more ecologically complicated than Regions 1 and 3, and therefore, a low sample size prevented LASSO from unraveling recruitment–environmental relationships. In other words, results suggest a spatial oceanographic gradient where Region 1 is more influenced by temperature and Region 3 is more influenced by wind. Therefore, Region 2 may represent a "hybrid" zone where both temperature and wind affect recruitment depending on the year. Because only 18 years were analyzed, LASSO was unable to tease apart such relationships.

While LASSO may have struggled with variable selection for Region 2, LASSO likely limited overfitting. Overfitting is not only a concern for fisheries-climate models, but is a particular concern in ecological studies with low sample sizes (Fox et al. 2015). While the present study fits into both categories, it is believed for numerous reasons, that overfitting risk was minimized and model performance was maximized in the present study. Not only did LASSO successfully reduce the number of variables for model construction consideration, but LASSO has previously been documented to reduce overfitting by providing more parsimonious variable selection, more specifically by reducing variance at the tradeoff of introducing bias (via the lambda value). GAMs also have been identified as a source of overfitting, as they may yield overly complex relationships (Wood and Augustin 2002). The model accuracy assessments employed in the present study indeed suggested possible GAM overfitting, thus causing linear models to be chosen for projections. Coupling LASSO with the employed model accuracy assessments that were based on resampling prediction scores (e.g., LOOCV procedures) has also previously been documented as an approach that minimizes overfitting (Stockwell and Peterson 2002; McNeish 2015). Therefore, minimized overfitting risks increase confidence of model performance. Furthermore, all the variables retained in the models chosen for projections contain possible mechanistic, ecological links to recruitment (see the next paragraphs). Not all studies that attempt to project fisheries production in response to climate variables identify clear links (Myers 1998). However, it is believed that by establishing distinct links that account for spatial variability (i.e., different links in different regions that correspond with spatial oceanographic gradients), the models in the present study may yield enhanced model performance. More specifically, accounting for a spatial gradient where one area may yield strong, negative relationships between the climate variable (e.g., SST) and fisheries production because that area is at the end of an environmental gradient (e.g., higher SST), but another area may yield no relationships between the climate variable and fisheries production because that area is in the middle of an environmental gradient, has been proposed to increase performance and limit the breakdown of such relationships

Table 2. Correlation coefficients of least absolute shrinkage and selection operator retained variables for each region.

Region 1		Region 2		Region 3	
Variables retained	Coefficient	Variables retained	Coefficient	Variables retained	Coefficient
FallT	−0.1730	N/A	N/A	SpringU	−0.1698
				WinterV	−0.1824
				SummerV	−0.1033

Table 3. Goodness of fit and prediction accuracy assessments for all candidate models including degrees of freedom (df), Akaike information criterion (AIC), leave-one-out cross-validation (LOOCV), and residual standard error (RSE) analyses.

Model	Variables	df	AIC	ModelR-squared	LOOCVR-squared	ModelRSE	LOOCVRSE	RSE %difference
Region 1								
Model 1*	FallT	16	47.661	0.269	0.130	0.775	0.901	16.25
Region 2								
Model 1	SummerU, WinterV, FallV, FallT	13	47.717	0.472	0.154	0.702	0.975	38.98
Model 2*	SummerU, WinterV, FallT	14	46.193	0.458	0.180	0.690	0.906	31.37
Model 3	SummerU, WinterV	15	45.679	0.412	0.169	0.693	0.872	25.92
Model 4	SummerU	16	46.267	0.320	0.164	0.734	0.831	12.85
Region 3								
Model 1	SpringU, WinterV, SummerV	14	37.992	0.5104	0.1659	0.612	0.840	37.10
Model 2	SpringU, WinterV	15	37.649	0.4632	0.1449	0.635	0.805	26.77
Model 3*	SpringU	16	39.069	0.3569	0.1909	0.639	0.725	13.47

*Denotes the model chosen for projections for each region.

4.2. Biogeographic patterns and mechanisms

Oceanographic gradients along the south shore of Long Island (LI) likely drive the observed biogeographic patterns in environment–recruitment relationships. Payne et al. (2017) suggests that identifying biogeographic patterns in environment–recruitment relationships may be key for obtaining accurate fisheries projections from environmental variables. Such patterns were observed in the present study, where recruitment in eastern waters is more influenced by wind patterns than that of western waters. This pattern is likely due to the lack of a major freshwater source influencing flow in Regions 2 and 3, whereas Region 1 may be more influenced by the Hudson River. In NYS waters, Zhang et al. (2009) found that the Hudson River plume can extend well into Region 1 waters. Chant et al. (2008) found that coastal chlorophyll concentrations in Region 1 match that of Upper New York Bay (1.6 gm C m^{-3}), whereas coastal chlorophyll concentrations in Regions 2 and 3 are lower (1.3 gm C m^{-3}). Therefore, in Region 1, wind influences may be subdued by that of the Hudson River, which may impact surfclam recruitment via affecting food quality and quantity. Furthermore, Vânia et al. (2014) found that in Portugal, catch of lagoon bivalve species (i.e., those more influenced by river output) is primarily driven by SST and catch of coastal bivalve species is more driven by wind patterns. Such a framework matches and provides further support for the proposed mechanisms driving the spatial patterns found in the present study.

Models yielded a negative relationship between FallT and CSI values in Regions 1 and 2, and no temperature relationship with CSI values in Region 3, likely due to the previously described oceanographic gradients. It is possible that in Regions 1 and 2, warmer fall temperatures yield direct metabolic stress on juvenile (i.e., recently settled) surfclams, resulting in poor recruitment. It is also possible that warmer fall temperatures increase predation pressure on juvenile surfclams, as predation is known to impact surfclam recruitment variability (Weissberger and Grassle 2003; Quijon et al. 2007). Warmer fall temperatures may not only increase metabolic rates of predators and therefore consumption rates of juvenile bivalves by predators (Miller 2013), but may also extend the season during which predators are consuming juvenile bivalves (Beukema and Dekker 2014). These mechanisms may explain historical recruitment trends; however, projections do not account for inherent mechanism nonstationarity. For example, ocean warming may cause Region 3 temperatures to eventually eclipse thermal thresholds, similar to Regions 1 and 2. Therefore, Region 3 may eventually yield a negative CSI–SST relationship, which may cause projections to lose accuracy through time due to extrapolations beyond the training range. While this possibility was taken into consideration and is in part why projections to 2100 were not attempted, future surfclam survey data would help in unraveling this potential nonstationarity.

Region 2 demonstrated a positive relationship between CSI and SummerU and Region 3 demonstrated a negative relationship with SpringU. These results suggest that winds blowing to the east result in better recruitment in western NYS waters and that winds blowing to the west result in better recruitment in eastern NYS waters. Given that Middle Atlantic Bight (MAB) surfclams spawn in June and July and that in the present study, SpringU includes June winds and SummerU includes July winds, it is possible that these relationships

Fig. 6. Observed (black lines) cohort strength index (CSI) trends from 1987 to 2004 and projected (gray lines) CSI trends from 1987 to 2019 from selected models (see Table 3) in Region 1 (A), Region 2 (B), and Region 3 (C). Arrows denote when Part 1 (CSIs projected from observed values) and Part 2 (CSIs projected from Coupled Model Intercomparison Project 6 projected values) projections begin. Shaded regions represent 95% confidence intervals.

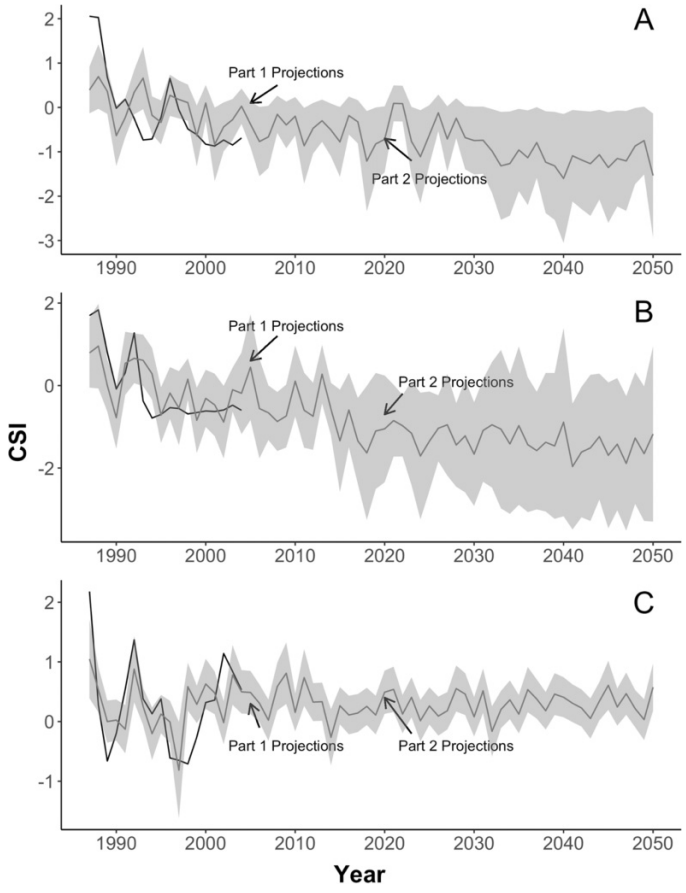

stem from wind-induced changes in larval transport and settlement locations. It is believed that larvae released in LI either settle in western LI, due to along-shore density-driven flow, or get transported to New Jersey (NJ) (Zhang et al. 2015). It is also believed that larvae that are released in Southern New England (SNE) either settle in SNE or get transported to eastern LI (Zhang et al. 2015). Therefore, established larvae dispersal patterns combined with the results of the present study support the idea that strong eastward winds may limit westward transport of larvae to NJ from LI, allowing more larvae to settle in western LI (Fig. S6), and that strong westward winds may allow increased transport of larvae to eastern LI from SNE, as opposed to those larvae being retained in SNE (Fig. S6). Previous field and biophysical modeling studies in the MAB have found that wind direction and speed can be linked to bivalve larvae settlement and recruitment due to similar larval transport mechanisms (Hart et al. 2020; Chen et al. 2021). Chen et al. (2021) also found that stronger northeasterly winds increased along-shore transport of scallop larvae in the MAB, providing support for the hypothesis that in the New York Bight (a subsection of the MAB), stronger easterly winds may increase transport of surfclam larvae from LI to NJ waters.

Food supply is also known to be a significant driver in interannual variation in shellfish recruitment (Carloni et al. 2018). Vânia et al. (2014) proposed that wind patterns may affect recruitment by influencing food supply for larvae and adults experiencing gametogenesis. Such a mechanism may explain why WinterV was retained in the best-fit model for Region 2 and selected for by LASSO in Region 3. More specifically, changes in the onset and intensity of the spring bloom leading to changes in food supply may explain the link between WinterV and recruitment. Henson et al. (2006) found that in the north Atlantic, stronger winter winds delay the spring bloom (via delayed stratification) to late May and June, at the end of surfclam gametogenesis and start of spawning. The present study found that stronger WinterV winds are linked to higher CSI values. Therefore, it is possible that stronger winter winds increase surfclam recruitment by delaying the bloom and increasing food availability during gametogenesis for spawning adults. Saba et al. (2015) also found that stronger winter winds correlated with higher spring chlorophyll concentrations in Georges Bank, providing further evidence for the idea that winter winds may project surfclam recruitment via indirect food supply links. A similar mechanism offers an additional explanation for CSI relationships with Spring and Summer winds, as Spring wind patterns have also been linked to chlorophyll production in NYS waters (Stegmann and Ullman 2004). Previous studies have successfully linked wind patterns to bivalve recruitment variability via food supply links (Fournier et al. 2012; Daewel et al. 2015), potentially via enhanced gametogenesis. It should be noted that the present study treats temperature and wind as separate variables. In coastal waters in the NYB, however, wind-induced upwelling can lead to lower temperatures, suggesting temperature and wind can be correlated (Yankovsky and Garvine 1998). Results suggest this link may be important, as positive SummerU winds led to higher CSI values (Region 2). In theory, more positive SummerU winds should lead to upwelling in NYS waters, and therefore cooler (and more physiologically tolerable) temperatures for surfclams. However, LASSO accounts for correlated variables, including direct measures of upwelling/downwelling as predictor variables may better relate or separate temperature and wind effects. Unfortunately, the low sample size in the present study limited inclusion of additional predictor variables, but future surfclam surveys would allow for higher degrees of freedom and therefore allow for inclusion of additional predictor variables (e.g., upwelling).

4.3. Projections and uncertainty

Studies that project marine ecosystem production metrics (e.g., fisheries recruitment) from climate–recruitment relationships typically suffer from significant uncertainty, potentially due to biased climate projections (Punt et al. 2014; Cheung et al. 2016). The present study addresses that criticism by using higher resolution from multiple models and therefore less biased climate projections. In addition, using

CMIP6 GCM output over that of CMIP5 may be especially important for fisheries projections in the north Atlantic and elsewhere, because CMIP6 output yields less biased SST projections (Li et al. 2020; Borchert et al. 2021). Additionally, CMIP5 output from CESM1-CAM5 and FGAOLS (two of the climate models used in the present study) have demonstrated relatively high, relative forecasting accuracy for SST and wind vectors (Li et al. 2013; Li et al. 2014; Halder et al. 2021). Furthermore, use of CMIP6 GCM output with enhanced spatial resolution likely increases model precision because previous results relied on statistical downscaling, which although sometimes beneficial, is also prone to increased uncertainty (Dimitrijevic and Laprise 2005; Pielke and Wilby 2012; Sunyer et al. 2012). It is the hope of these authors that using CMIP6 GCM output, as was done in the present study, will represent the new standard of fisheries projections under climate change scenarios.

Although CMIP6 projections yield a slight increase in recruitment in Region 3, Regions 1 and 2 both exhibited negative relationships with FallT and yielded projections of a 100% decline in recruitment by 2050. GCM output projected an increase in Fall SST of approximately 0.5 °C per decade in NYS waters. Although this is relatively high for other coastal regions in the north Atlantic (Villarino et al. 2015), it is comparable to other reports of increasing Fall SST trends in the MAB (Wallace et al. 2018). If an SSP2 (equivalent to RCP4.5) was used, it is possible that projected surfclam recruitment may yield lower declines in western waters, as SSP2 would yield lower SST increases (~1 °C in the north Atlantic by 2050) (Khan et al. 2013; Fischer 2015). Speculating on different outcomes under different SSP scenarios represents just one type of uncertainty in considering fisheries-climate projections. Model uncertainty and internal variability should also be considered when making projections (Cheung et al. 2016). The present study attempted to account for model uncertainty by using multiple GCMs, choosing GCMs that had previously been compared to observed data (e.g., Voldoire et al. 2019) and choosing GCMs with the highest spatial resolution. However, model uncertainty cannot be eliminated, especially for Regions 2 and 3, as these regions used wind projections and only three GCMs. Furthermore, the models in the present study likely missed internal ecological variability, potentially limiting projection precision. For example, predation impacts surfclam recruitment but predation was not included in models and projections. Future work may use ecosystem level models (e.g., Ecopath with Ecosim) to create projections that may better account for internal ecological variability.

5. Conclusions

Broadly speaking, the models developed here suggest that surfclam recruitment will decrease in western NYS waters due to rising SST and slight increase in eastern NYS waters due to changing wind patterns. New surfclam surveys would be crucial in validating models, particularly in eastern NYS waters where nonstationarity may alter the recruitment–temperature relationships. However, as of 2019, local surfclam fishermen almost exclusively fish in eastern NYS waters because they are unable to find enough surfclams in western NYS (Region 1) waters to financially support fishing trips. Although anecdotal, such information supports the observed relationships and projections. Multiple experimental and field studies support the discussed thermally induced mechanisms, but additional field studies regarding surfclam larvae, recently settled surfclam larvae, and food sources are needed to explain the underlying hydrodynamic mechanisms behind the observed recruitment–wind relationships. Additionally, biophysical modeling studies with sensitivity analyses to examine the degree to which wind can affect larval transport patterns would provide insight regarding recruitment–wind relationships. Nevertheless, the present study not only provided the first long-term quantification and projection of surfclam recruitment using updated climate projections but also found longitudinal spatial patterns in recruitment and related temporal patterns in recruitment to climate variables. These relationships and their projections may improve strategic management of the surfclam fishery. Additionally, the present study provided an updated method (i.e., a region-specific, semiautomated variable and model selection process) for fisheries recruitment–climate modeling that yielded reasonably high predictive accuracy and will therefore hopefully serve as a template for future studies that aim to project recruitment in response to climate change for other temperate, coastal species.

Acknowledgements

We genuinely thank the New York State Department of Environmental Conservation for sharing survey data.

Article information

History dates

Received: 2 May 2022
Accepted: 23 January 2023
Accepted manuscript online: 15 February 2023
Version of record online: 20 March 2023

Data availability

Data are available upon request.

Author information

Author ORCIDs

Daniel Hennen https://orcid.org/0000-0003-1819-2402

Author contributions

Conceptualization: EP-E, BA

Data curation: RCJ, DH, JO
Formal analysis: RCJ, DH, RC, KL
Funding acquisition: BA
Investigation: RCJ, RC, JO
Methodology: RCJ, DH, RC, KL, JO
Project administration: BA
Resources: RC, EP-E, JO
Software: RCJ, DH, RC, KL
Validation: RCJ, DH, RC, KL
Visualization: RCJ, DH, KL
Writing – original draft: RCJ
Writing – review & editing: RCJ, DH, RC, KL, EP-E, JO, BA

Competing interests

The authors declare that there are no competing interests.

Funding information

Financial support was provided by the New York Ocean Action Plan via New York Sea Grant (Grant No. R/FBF-39).

Supplementary material

Supplementary data are available with the article at https://doi.org/10.1139/cjfas-2022-0091.

References

A'mar, Z.T., Punt, A.E., and Dorn, M.W. 2009. The evaluation of two management strategies for the Gulf of Alaska walleye pollock fishery under climate change. ICES J. Mar. Sci. **66**(7): 1614–1632. doi:10.1093/icesjms/fsp044.

Anderson, D., and Burnham, K. 2004. Model selection and multi-model inference. 2nd ed. Springer-Verlag, New York, NY.

Bartolino, V., Margonski, P., Lindegren, M., Linderholm, H.W., Cardinale, M., Rayner, D., et al. 2014. Forecasting fish stock dynamics under climate change: Baltic herring (*Clupea harengus*) as a case study. Fish. Oceanogr. **23**(3): 258–269. doi:10.1111/fog.12060.

Bell, R.J., Wood, A., Hare, J., Richardson, D., Manderson, J., and Miller, T. 2018. Rebuilding in the face of climate change. Can. J. Fish. Aquat. Sci. **75**(9): 1405–1414. doi:10.1139/cjfas-2017-0085.

Beukema, J., and Dekker, R. 2014. Variability in predator abundance links winter temperatures and bivalve recruitment: correlative evidence from long-term data in a tidal flat. Mar. Ecol. Prog. Ser. **513**: 1–15. doi:10.3354/meps10978.

Borchert, L.F., Menary, M.B., Swingedouw, D., Sgubin, G., Hermanson, L., and Mignot, J. 2021. Improved decadal predictions of North Atlantic subpolar gyre SST in CMIP6. Geophys. Res. Lett. **48**(3): e2020GL091307. doi:10.1029/2020GL091307.

Boyce, D.G., Lewis, M.R., and Worm, B. 2010. Global phytoplankton decline over the past century. Nature, **466**(7306): 591–596. doi:10.1038/nature09268. PMID: 20671703.

Brander, K. 2010. Impacts of climate change on fisheries. J. Mar. Syst. **79**(3–4): 389–402. doi:10.1016/j.jmarsys.2008.12.015.

Brosset, P., Smith, A.D., Plourde, S., Castonguay, M., Lehoux, C., and Van Beveren, E. 2020. A fine-scale multi-step approach to understand fish recruitment variability. Sci. Rep. **10**(1): 1–14. doi:10.1038/s41598-020-73025-z. PMID: 31913322.

Brunel, T., and Boucher, J. 2007. Long-term trends in fish recruitment in the north-east Atlantic related to climate change. Fish. Oceanogr. **16**(4): 336–349. doi:10.1111/j.1365-2419.2007.00435.x.

Caputi, N., Melville-Smith, R., de Lestang, S., Pearce, A., and Feng, M. 2010. The effect of climate change on the western rock lobster (*Panulirus cygnus*) fishery of Western Australia. Can. J. Fish. Aquat. Sci. **67**(1): 85–96. doi:10.1139/F09-167.

Carloni, J.T., Wahle, R., Geoghegan, P., and Bjorkstedt, E. 2018. Bridging the spawner-recruit disconnect: trends in American lobster recruitment linked to the pelagic food web. Bull. Mar. Sci. **94**(3): 719–735. doi:10.5343/bms.2017.1150.

Chant, R.J., Wilkin, J., Zhang, W., Choi, B.-J., Hunter, E., Castelao, R., et al. 2008. Dispersal of the Hudson River plume in the New York Bight: synthesis of observational and numerical studies during LaTTE. Oceanography, **21**(4): 148–161. doi:10.5670/oceanog.2008.11.

Chen, C., Zhao, L., Gallager, S., Ji, R., He, P., Davis, C., et al. 2021. Impact of larval behaviors on dispersal and connectivity of sea scallop larvae over the northeast US shelf. Prog. Oceanogr. **195**: 102604. doi:10.1016/j.pocean.2021.102604.

Cheung, W.W., Frölicher, T.L., Asch, R.G., Jones, M.C., Pinsky, M.L., Reygondeau, G., et al. 2016. Building confidence in projections of the responses of living marine resources to climate change. ICES J. Mar. Sci. **73**(5): 1283–1296. doi:10.1093/icesjms/fsv250.

Chintala, M., and Grassle, J. 2001. Comparison of recruitment frequency and growth of surfclams, *Spisula solidissima* (Dillwyn, 1817), in different inner-shelf habitats of New Jersey. J. Shellfish Res. **20**(3): 1177–1186.

Churchill, J.H., Runge, J., and Chen, C. 2011. Processes controlling retention of spring-spawned Atlantic cod (*Gadus morhua*) in the western Gulf of Maine and their relationship to an index of recruitment success. Fish. Oceanogr. **20**(1): 32–46. doi:10.1111/j.1365-2419.2010.00563.x.

Daewel, U., Schrum, C., and Gupta, A.K. 2015. The predictive potential of early life stage individual-based models (IBMs): an example for Atlantic cod *Gadus morhua* in the North Sea. Mar. Ecol. Prog. Ser. **534**: 199–219. doi:10.3354/meps11367.

Dahl, S., and Hornstein, J. 2010. 2008 Atlantic Ocean Surfclam Population Assessment Survey. New York State Department of Environmental Conservation. pp. 1–69.

Dahlgren, J.P. 2010. Alternative regression methods are not considered in Murtaugh (2009) or by ecologists in general. Ecol. Lett. **13**(5): E7–E9. doi:10.1111/j.1461-0248.2010.01460.x. PMID: 20529100.

Deyle, E.R., Fogarty, M., Hsieh, C.-H., Kaufman, L., MacCall, A.D., Munch, S.B., et al. 2013. Predicting climate effects on Pacific sardine. Proc. Natl. Acad. Sci. U.S.A. **110**(16): 6430–6435. doi:10.1073/pnas.1215506110. PMID: 23536299.

Dickey-Collas, M., Payne, M.R., Trenkel, V.M., and Nash, R.D. 2014. Hazard warning: model misuse ahead. ICES J. Mar. Sci. **71**(8): 2300–2306. doi:10.1093/icesjms/fst215.

Dimitrijevic, M., and Laprise, R. 2005. Validation of the nesting technique in a regional climate model and sensitivity tests to the resolution of the lateral boundary conditions during summer. Clim. Dyn. **25**(6): 555–580. doi:10.1007/s00382-005-0023-6.

Fauchald, P., Arneberg, P., Debernard, J.B., Lind, S., Olsen, E., and Hausner, V.H. 2021. Poleward shifts in marine fisheries under Arctic warming. Environ. Res. Lett. **16**(7): 074057. doi:10.1088/1748-9326/ac1010.

Fischer, M. 2015. Changes in the predictability of the North Atlantic ocean under global warming. Staats-und Universitätsbibliothek Hamburg Carl von Ossietzky.

Flanagan, A., and Cerrato, R. 2015. An approach for quantifying the efficacy of ecological classification schemes as management tools. Cont. Shelf Res. **109**: 55–66. doi:10.1016/j.csr.2015.08.023.

Fournier, J., Levesque, E., Pouvreau, S., Le Pennec, M., and Le Moullac, G. 2012. Influence of plankton concentration on gametogenesis and spawning of the black lip pearl oyster *Pinctada margaritifera* in Ahe atoll lagoon (Tuamotu archipelago, French polynesia). Mar. Pollut. Bull. **65**(10–12): 463–470. doi:10.1016/j.marpolbul.2012.03.027. PMID: 22560741.

Fox, G.A., Negrete-Yankelevich, S., and Sosa, V.J. 2015. Ecological statistics: contemporary theory and application. Oxford University Press, USA.

Gownaris, N.J., Rountos, K.J., Kaufman, L., Kolding, J., Lwiza, K.M., and Pikitch, E.K. 2018. Water level fluctuations and the ecosystem functioning of lakes. J. Great Lakes Res. **44**(6): 1154–1163. doi:10.1016/j.jglr.2018.08.005.

Guisan, A., and Zimmermann, N.E. 2000. Predictive habitat distribution models in ecology. Ecol. Modell. **135**(2–3): 147–186. doi:10.1016/S0304-3800(00)00354-9.

Halder, S., Parekh, A., Chowdary, J.S., Gnanaseelan, C., and Kulkarni, A. 2021. Assessment of CMIP6 models' skill for tropical Indian Ocean sea surface temperature variability. Int. J. Climatol. **41**(4): 2568–2588. doi:10.1002/joc.6975.

Hare, J.A., Brooks, E.N., Palmer, M.C., and Churchill, J.H. 2015. Re-evaluating the effect of wind on recruitment in Gulf of Maine Atlantic Cod (*Gadus morhua*) using an environmentally-explicit stock recruitment model. Fish. Oceanogr. **24**(1): 90–105. doi:10.1111/fog.12095.

Harley, C.D., Randall Hughes, A., Hultgren, K.M., Miner, B.G., Sorte, C.J., Thornber, C.S., et al. 2006. The impacts of climate change in coastal marine systems. Ecol. Lett. **9**(2): 228–241. doi:10.1111/j.1461-0248.2005.00871.x. PMID: 16958887.

Hart, D.R., Munroe, D.M., Caracappa, J.C., Haidvogel, D., Shank, B.V., Rudders, D.B., et al. 2020. Spillover of sea scallops from rotational closures in the Mid-Atlantic Bight (United States). ICES J. Mar. Sci. **77**(5): 1992–2002. doi:10.1093/icesjms/fsaa099.

Hastie, T., Tibshirani, R., and Friedman, J. 2009. The elements of statistical learning. Springer.

Hegyi, G., and Garamszegi, L.Z. 2011. Using information theory as a substitute for stepwise regression in ecology and behavior. Behav. Ecol. Sociobiol. **65**(1): 69–76. doi:10.1007/s00265-010-1036-7.

Henson, S.A., Robinson, I., Allen, J.T., and Waniek, J.J. 2006. Effect of meteorological conditions on interannual variability in timing and magnitude of the spring bloom in the Irminger Basin, North Atlantic. Deep-Sea Res., Part I. **53**(10): 1601–1615. doi:10.1016/j.dsr.2006.07.009.

Ho, C.K., Stephenson, D.B., Collins, M., Ferro, C.A., and Brown, S.J. 2012. Calibration strategies: a source of additional uncertainty in climate change projections. Bull. Am. Meteorol. Soc. **93**(1): 21–26. doi:10.1175/2011BAMS3110.1.

Holmes, E. 2020. SardineForecast. University of Washington.

Hornstein, J., Espinosa, E.P., Cerrato, R.M., Lwiza, K.M., and Allam, B. 2018. The influence of temperature stress on the physiology of the Atlantic surfclam, *Spisula solidissima*. Comp. Biochem. Physiol. A Mol. Integr. Physiol. **222**: 66–73. doi:10.1016/j.cbpa.2018.04.011.

IPCC. 2014. Climate change 2014: impacts, adaptation, and vulnerability. Part B: regional aspects. Cambridge University Press, Cambridge, UK.

Keyl, F., and Wolff, M. 2008. Environmental variability and fisheries: what can models do? Rev. Fish Biol. Fish. **18**(3): 273–299. doi:10.1007/s11160-007-9075-5.

Khan, A.H., Levac, E., and Chmura, G.L. 2013. Future sea surface temperatures in Large Marine Ecosystems of the Northwest Atlantic. ICES J. Mar. Sci. **70**(5): 915–921. doi:10.1093/icesjms/fst002.

Kidd, A.C., McGettrick, M., Tsim, S., Halligan, D.L., Bylesjo, M., and Blyth, K.G. 2018. Survival prediction in mesothelioma using a scalable Lasso regression model: instructions for use and initial performance using clinical predictors. BMJ Open Respir. Res. **5**(1): e000240. doi:10.1136/bmjresp-2017-000240. PMID: 29468073.

Kim, Y., and Powell, E.N. 2004. Surfclam histopathology survey along the Delmarva mortality line. J. Shellfish Res. **23**(2): 429–442.

Koenigk, T., Fuentes-Franco, R., Meccia, V., Gutjahr, O., Jackson, L.C., New, A.L., et al. 2020. Deep water formation in the North Atlantic Ocean in high resolution global coupled climate models. Ocean Sci. Discuss. 1–39.

Koul, V., Sguotti, C., Årthun, M., Brune, S., Düsterhus, A., Bogstad, B., et al. 2021. Skilful prediction of cod stocks in the North and Barents Sea a decade in advance. Commun. Earth Environ. **2**(1): 1–10.

Kuhn, M. 2008. Caret package. J. Stat. Softw. **28**(5).

Kumar, S., Attri, S., and Singh, K. 2019. Comparison of Lasso and stepwise regression technique for wheat yield prediction. J. Agrometeorol. **21**(2): 188–192. doi:10.54386/jam.v21i2.231.

Le Bris, A., Mills, K.E., Wahle, R.A., Chen, Y., Alexander, M.A., Allyn, A.J., et al. 2018. Climate vulnerability and resilience in the most valuable North American fishery. Proc. Natl. Acad. Sci. U.S.A. **115**(8): 1831–1836. doi:10.1073/pnas.1711122115.

Lehodey, P., Senina, I., Calmettes, B., Hampton, J., and Nicol, S. 2013. Modelling the impact of climate change on Pacific skipjack tuna population and fisheries. Clim. Change, **119**(1): 95–109. doi:10.1007/s10584-012-0595-1.

Lehodey, P., Senina, I., Nicol, S., and Hampton, J. 2015. Modelling the impact of climate change on South Pacific albacore tuna. Deep Sea Res., Part II. **113**: 246–259. doi:10.1016/j.dsr2.2014.10.028.

Li, J.L., Lee, W.L., Waliser, D., David Neelin, J., Stachnik, J.P., and Lee, T. 2014. Cloud-precipitation-radiation-dynamics interaction in global climate models: a snow and radiation interaction sensitivity experiment. J. Geophys. Res. Atmos. **119**(7): 3809–3824. doi:10.1002/2013JD021038.

Li, L., Lin, P., Yu, Y., Wang, B., Zhou, T., Liu, L., et al. 2013. The flexible global ocean-atmosphere-land system model, Grid-point Version 2: FGOALS-g2. Adv. Atmos. Sci. **30**(3): 543–560. doi:10.1007/s00376-012-2140-6.

Li, L., Yu, Y., Tang, Y., Lin, P., Xie, J., Song, M., et al. 2020. The flexible global ocean-atmosphere-land system model grid-point version 3 (FGOALS-g3): description and evaluation. J. Adv. Model. Earth Syst. **12**(9): e2019MS002012. doi:10.1029/2019MS002012.

Li, W., Feng, J., and Jiang, T. 2011. IsoLasso: a LASSO regression approach to RNA-Seq based transcriptome assembly. J. Comput. Biol. **18**(11): 1693–1707. doi:10.1089/cmb.2011.0171.

Lu, Y., Zhou, Y., Qu, W., Deng, M., and Zhang, C. 2011. A Lasso regression model for the construction of microRNA-target regulatory networks. Bioinformatics, **27**(17): 2406–2413. doi:10.1093/bioinformatics/btr410.

Ma, H. 2005. Spatial and temporal variation in surfclam (*Spisula solidissima*) larval supply and settlement on the New Jersey inner shelf during summer upwelling and downwelling. Estuar. Cost. Shelf Sci. **62**(1–2): 41–53. doi:10.1016/j.ecss.2004.08.005.

Ma, H., and Grassle, J.P. 2004. Invertebrate larval availability during summer upwelling and downwelling on the inner continental shelf off New Jersey. J. Mar. Res. **62**(6): 837–865. doi:10.1357/0022240042880882.

Ma, H., Grassle, J.P., and Rosario, J.M. 2006. Initial recruitment and growth of surfclams (Spisula solidissima Dillwyn) on the inner continental shelf of New Jersey. J. Shellfish Res. **25**(2): 481–489. doi:10.2983/0730-8000(2006)25%5b481:IRAGOS%5d2.0.CO;2.

Marzec, R.J., Kim, Y., and Powell, E.N. 2010. Geographical trends in weight and condition index of surfclams (*Spisula solidissima*) in the Mid-Atlantic Bight. J. Shellfish Res. **29**(1): 117–128. doi:10.2983/035.029.0104.

Maunder, M.N., and Thorson, J.T. 2019. Modeling temporal variation in recruitment in fisheries stock assessment: a review of theory and practice. Fish. Res. **217**: 71–86. doi:10.1016/j.fishres.2018.12.014.

McEligot, A.J., Poynor, V., Sharma, R., and Panangadan, A. 2020. Logistic LASSO regression for dietary intakes and breast cancer. Nutrients, **12**(9): 2652. doi:10.3390/nu12092652.

McNeish, D.M. 2015. Using Lasso for predictor selection and to assuage overfitting: a method long overlooked in behavioral sciences. Multivariate Behav. Res. **50**(5): 471–484. doi:10.1080/00273171.2015.1036965.

Miller, L.P. 2013. The effect of water temperature on drilling and ingestion rates of the dogwhelk Nucella lapillus feeding on Mytilus edulis mussels in the laboratory. Mar. Biol. **160**(6): 1489–1496. doi:10.1007/s00227-013-2202-z.

Miller, T.J., Hare, J.A., and Alade, L.A. 2016. A state-space approach to incorporating environmental effects on recruitment in an age-structured assessment model with an application to southern New England yellowtail flounder. Can. J. Fish. Aquat. Sci. **73**(8): 1261–1270. doi:10.1139/cjfas-2015-0339.

Muhling, B.A., Tommasi, D., Ohshimo, S., Alexander, M.A., and DiNardo, G. 2018. Regional-scale surface temperature variability allows prediction of Pacific bluefin tuna recruitment. ICES J. Mar. Sci. **75**(4): 1341–1352. doi:10.1093/icesjms/fsy017.

Munroe, D., Narváez, D., Hennen, D., Jacobson, L., Mann, R., Hofmann, E., et al. 2016. Fishing and bottom water temperature as drivers of change in maximum shell length in Atlantic surfclams (*Spisula solidissima*). Estuar. Cost. Shelf Sci. **170**: 112–122. doi:10.1016/j.ecss.2016.01.009.

Myers, R.A. 1998. When do environment–recruitment correlations work? Rev. Fish Biol. Fish. **8**(3): 285–305. doi:10.1023/A:1008828730759.

Nakata, H., Fujihara, M., Suenaga, Y., Nagasawa, T., and Fujii, T. 2000. Effect of wind blows on the transport and settlement of brown sole (*Pleuronectes herzensteini*) larvae in a shelf region of the Sea of Japan: numerical experiments with an Euler–Lagrangian model. J. Sea Res. **44**(1–2): 91–100. doi:10.1016/S1385-1101(00)00042-3.

Narváez, D.A., Munroe, D.M., Hofmann, E.E., Klinck, J.M., Powell, E.N., Mann, R., and Curchitser, E. 2015. Long-term dynamics in Atlantic surfclam (*Spisula solidissima*) populations: the role of bottom water temperature. J. Mar. Syst. **141**: 136–148. doi:10.1016/j.jmarsys.2014.08.007.

NEFSC. 2017. 61st Northeast Regional Stock Assessment Workshop (61st SAW) Assessment Report. U.S. Department of Commerce, Northeast Fisheries Science Center Reference Document 17-05.

O'Dwyer, J., and Hornstein, J. 2013. 2012 Atlantic Ocean Surfclam Population Assessment. New York State Department of Environmental Conservation.

O`Reilly, J.E., and Zetlin, C.A. 1998. Seasonal, horizontal, and vertical distribution of phytoplankton chlorophyll a in the northeast US continental shelf ecosystem. NOAA Technical Report NMFS.

Olden, J.D., and Jackson, D.A. 2000. Torturing data for the sake of generality: how valid are our regression models? Ecoscience, **7**(4): 501–510. doi:10.1080/11956860.2000.11682622.

Pawlowicz, R. 2020. M_Map: a mapping package for MATLAB, version 1.4 m. Available from http://www.eoas.ubc.ca/~rich/map.html.

Payne, M.R., Hobday, A.J., MacKenzie, B.R., Tommasi, D., Dempsey, D.P., Fässler, S.M., et al. 2017. Lessons from the first generation of marine ecological forecast products. Front. Mar. Sci. **4**: 289.

,Pielke, R.A., Sr, and Wilby, R.L. 2012. Regional climate downscaling: what's the point? EOS, Trans., Am. Geophys. Union, **93**(5): 52–53. doi:10.1029/2012EO050008.

Planque, B., and Frédou, T. 1999. Temperature and the recruitment of Atlantic cod (*Gadus morhua*). Can. J. Fish. Aquat. Sci. **56**(11): 2069–2077. doi:10.1139/f99-114.

Plumpton, H. 2018. Black Scoter (Melanitta americana) winter habitat use and movement patterns along the Atlantic Coast of the United States. Clemson University. A thesis presented to the Graduate School of Clemson University.

Punt, A.E., A'mar, T., Bond, N.A., Butterworth, D.S., de Moor, C.L., De Oliveira, J.A., et al. 2014. Fisheries management under climate and environmental uncertainty: control rules and performance simulation. ICES J. Mar. Sci. **71**(8): 2208–2220. doi:10.1093/icesjms/fst057.

Quijon, P.A., Grassle, J., and Rosario, J. 2007. Naticid snail predation on early post-settlement surfclams (Spisula solidissima) on the inner continental shelf of New Jersey, USA. Mar. Biol. **150**(5): 873–882. doi:10.1007/s00227-006-0399-9.

R Core Team. 2020. R: a language and environment for statistical computing. R Foundation for Statistical Computing, Vienna, Austria.

Rheuban, J.E., Kavanaugh, M.T., and Doney, S.C. 2017. Implications of future northwest Atlantic bottom temperatures on the American lobster (*Homarus americanus*) fishery. J. Geophys. Res. Oceans, **122**(12): 9387–9398. doi:10.1002/2017JC012949.

Riahi, K., Rao, S., Krey, V., Cho, C., Chirkov, V., Fischer, G., et al. 2011. RCP 8.5: a scenario of comparatively high greenhouse gas emissions. Clim. Change, **109**(1): 33–57. doi:10.1007/s10584-011-0149-y.

Saba, V.S., Griffies, S.M., Anderson, W.G., Winton, M., Alexander, M.A., Delworth, T.L., et al. 2016. Enhanced warming of the Northwest Atlantic Ocean under climate change. J. Geophys. Res. Oceans, **121**(1): 118–132. doi:10.1002/2015JC011346.

Saba, V.S., Hyde, K.J., Rebuck, N.D., Friedland, K.D., Hare, J.A., Kahru, M., and Fogarty, M.J. 2015. Physical associations to spring phytoplankton biomass interannual variability in the US Northeast Continental Shelf. J. Geophys. Res. Biogeosci. **120**(2): 205–220. doi:10.1002/2014JG002770.

Séférian, R., Berthet, S., Yool, A., Palmieri, J., Bopp, L., Tagliabue, A., et al. 2020. Tracking improvement in simulated marine biogeochemistry between CMIP5 and CMIP6. Curr. Clim. Change Rep. 1–25.

Skagseth, Ø., Slotte, A., Stenevik, E.K., and Nash, R.D. 2015. Characteristics of the Norwegian Coastal Current during years with high recruitment of Norwegian spring spawning herring (*Clupea harengus* L.). PLoS ONE, **10**(12): e0144117. doi:10.1371/journal.pone.0144117.

South, A. 2023. naturalearthhires: high resolution world vector map data from natural earth used in rnaturalearth. Available from https://github.com/ropensci/rnaturalearthhires.

Stegmann, P., and Ullman, D. 2004. Variability in chlorophyll and sea surface temperature fronts in the Long Island Sound outflow region from satellite observations. J. Geophys. Res. Oceans, **109**(C7). doi:10.1029/2003JC001984.

Stockwell, D.R., and Peterson, A.T. 2002. Effects of sample size on accuracy of species distribution models. Ecol. Modell. **148**(1): 1–13. doi:10.1016/S0304-3800(01)00388-X.

Sunyer, M., Madsen, H., and Ang, P. 2012. A comparison of different regional climate models and statistical downscaling methods for extreme rainfall estimation under climate change. Atmos. Res. **103**: 119–128. doi:10.1016/j.atmosres.2011.06.011.

Szuwalski, C., Cheng, W., Foy, R., Hermann, A.J., Hollowed, A., Holsman, K., et al. 2021. Climate change and the future productivity and distribution of crab in the Bering Sea. ICES J. Mar. Sci. **78**(2): 502–515. doi:10.1093/icesjms/fsaa140.

Testa, G., Neira, S., Giesecke, R., and Piñones, A. 2022. Projecting environmental and krill fishery impacts on the Antarctic Peninsula food web in 2100. Prog. Oceanogr. **206**: 102862. doi:10.1016/j.pocean.2022.102862.

Tian, Y., Akamine, T., and Suda, M. 2003. Variations in the abundance of Pacific saury (*Cololabis saira*) from the northwestern Pacific in relation to oceanic-climate changes. Fish. Res. **60**(2–3): 439–454. doi:10.1016/S0165-7836(02)00143-1.

Tibshirani, R. 1996. Regression shrinkage and selection via the Lasso. J. R. Stat. Soc. Ser. B Methodol. **58**(1): 267–288.

Vânia, B., Ullah, H., Teixeira, C.M., Range, P., Erzini, K., and Leitão, F. 2014. Influence of environmental variables and fishing pressure on bivalve fisheries in an inshore lagoon and adjacent nearshore coastal area. Estuar. Coast. **37**(1): 191–205. doi:10.1007/s12237-013-9658-4.

Vikebø, F.B., Strand, K.O., and Sundby, S. 2019. Wind intensity is key to phytoplankton spring bloom under climate change. Front. Mar. Sci. **6**: 518. doi:10.3389/fmars.2019.00518.

Villarino, E., Chust, G., Licandro, P., Butenschön, M., Ibaibarriaga, L., Larrañaga, A., and Irigoien, X. 2015. Modelling the future biogeography of North Atlantic zooplankton communities in response to climate change. Mar. Ecol. Prog. Ser. **531**: 121–142. doi:10.3354/meps11299.

Voldoire, A. Saint-Martin, D. Senesi, S. Decharme, B. Alias, A. Chevallier, M. et al. 2019. Evaluation of CMIP6 DECK Experiments With CNRM-CM6-1. J. Adv. Model. Earth Syst., **11** (7):2177–2213. doi:10.1029/2019MS001683.

Wallace, E.J., Looney, L.B., and Gong, D. 2018. Multi-decadal trends and variability in temperature and salinity in the Mid-Atlantic Bight, Georges Bank, and Gulf of Maine. J. Mar. Res. **76**(5): 163–215. doi:10.1357/002224018826473281.

Wang, T., and Wang, Y. 2020. Behavioral responses to ocean acidification in marine invertebrates: new insights and future directions. J. Oceanol. Limnol. **38**(3): 759–772. doi:10.1007/s00343-019-9118-5.

Weinberg, J. 1999. Age-structure, recruitment, and adult mortality in populations of the Atlantic surfclam, *Spisula solidissima*, from 1978 to 1997. Mar. Biol. **134**(1): 113–125. doi:10.1007/s002270050530.

Weinberg, J.R. 2005. Bathymetric shift in the distribution of Atlantic surfclams: response to warmer ocean temperature. ICES J. Mar. Sci. **62**(7): 1444–1453. doi:10.1016/j.icesjms.2005.04.020.

Weissberger, E., and Grassle, J. 2003. Settlement, first-year growth, and mortality of surfclams, Spisula solidissima. Estuarine, Coastal Shelf Sci. **56**(3–4): 669–684. doi:10.1016/S0272-7714(02)00218-4.

Wessel, P., and Smith, W. 2017. A global self-consistent, hierarchical, high-resolution geography database. Available from https://www.soest.hawaii.edu/pwessel/gshhg/.

Whittingham, M.J., Stephens, P.A., Bradbury, R.B., and Freckleton, R.P. 2006. Why do we still use stepwise modelling in ecology and behaviour? J. Anim. Ecol. **75**(5): 1182–1189. doi:10.1111/j.1365-2656.2006.01141.x.

Wigley, R.L., and Emery, K. 1968. Submarine photos of commercial shellfish off northeastern United States. Commer. Fish. Rev. **30**(3): 43–49.

Winder, M., and Sommer, U. 2012. Phytoplankton response to a changing climate. Hydrobiologia, **698**(1): 5–16. doi:10.1007/s10750-012-1149-2.

Wolff, M., and Vargas, J. 1994. RV Victor Hensen Costa Rica Expedition 1993/1994 Cruise Report, Bremen, ZMT.

Wood, S.N., and Augustin, N.H. 2002. GAMs with integrated model selection using penalized regression splines and applications to environmental modelling. Ecol. Modell. **157**(2–3): 157–177. doi:10.1016/S0304-3800(02)00193-X.

Yankovsky, A.E., and Garvine, R.W. 1998. Subinertial dynamics on the inner New Jersey shelf during the upwelling season. J.

Phys. Oceanogr. **28**(12): 2444–2458. doi:10.1175/1520-0485(1998)028%3c2444:SDOTIN%3e2.0.CO;2.

Zhang, W.G.,Wilkin,, J.L., and Chant, R.J. 2009. Modeling the pathways and maean dynamics of river plume dispersal in the New York Bight. J. Phys. Oceanogr. **39**(5): 1167–1183. doi:10.1175/2008JPO4082.1.

Zhang, X., Haidvogel, D., Munroe, D., Powell, E.N., Klinck, J., Mann, R., and Castruccio, F.S. 2015. Modeling larval connectivity of the Atlantic surfclams within the Middle Atlantic Bight: model development, larval dispersal and metapopulation connectivity. Estuar. Coast. Shelf Sci. **5** (153):38–55. doi:10.1016/j.ecss.2014.11.033.